AIChE

Effect of Sample Size on Microwave Power Absorption Within Dielectric Materials: 2D Numerical Results vs. Closed-Form Expressions

S. Curet, O. Rouaud, and L. Boillereaux
Dept. of Food Engineering, ENITIAA, GEPEA-UMR CNRS 6144, 44322 Nantes Cedex 3, France

DOI 10.1002/aic.11774
Published online April 28, 2009 in Wiley InterScience (www.interscience.wiley.com).

This study deals with the analytical and numerical solutions of the heat source term because of microwave heating for high and low dielectric materials in 1D and 2D configurations. The authors compare closed-form expressions dedicated to microwave power calculation to numerical simulations. A comprehensive and accurate analysis of the microwave power reflected from the surface of the sample is also carried out during microwave heating. The influence of sample length is studied using an original numerical procedure. The study highlights that 1D closed-form expressions can be extended to 2D configurations in the case of sufficiently high dielectric properties. Examples of heating rate during 2D microwave heating in TE_{10} mode are finally presented. © 2009 American Institute of Chemical Engineers *AIChE J,* 55: 1569–1583, 2009
Keywords: heat transfer, food, mathematical modeling

Introduction

In many industrial processes, microwaves can be used as heat source because of their ability to considerably shorten the heating process. The most important applications concern food tempering, baking and cooking, the pasteurization, the drying, the preheating for rubber vulcanization, and also the processing of polymers or minerals.[1] The temperature distribution inside materials heated by microwaves depends on their dielectric properties, which influence the distribution of the absorbed energy. The size and shape of the processed material are also an important parameter. The complexity of the heating pattern is particularly obvious within multicomponent materials[2,3] or when phase changes occur during the process.[4–6] The heterogeneity of temperature is indeed reinforced when the dielectric properties experience an abrupt increase after a certain temperature rise, leading to thermal runaway and the possible damage of products. To predict the occurrence of such hot spots and to prevent it, it is necessary to develop easy-to-use mathematical models.

Thermal modeling can be very useful to optimize microwave processes; however, the heat source term calculation remains the main difficulty. Regarding literature, microwave heating can be modeled using two main approaches. The simplest one is called ''Lambert's law'' and assumes an exponential decay of the microwave absorbed power as a function of the penetration depth within the sample. This model is valid for semi-infinite mediums or under specific operating conditions.[7–10] The most rigorous method is based on the complete resolution of Maxwell's equations, which govern the propagation of the electromagnetic field. This approach is the only one that describes the resonance phenomena because of constructive interference of traveling waves inside the medium. A great number of publications, including numerical aspects of the resolution of such nonlinear equations, are devoted to this issue.[11–16] Despite the constant increase of computational resources, this approach, coupled with the resolution of the heat equation, remains very time-consuming especially for 2D or 3D configurations. To reduce the detrimental computational times and describe the

Correspondence concerning this article should be addressed to O. Rouaud at olivier.rouaud@enitiaa-nantes.fr

complex behavior of samples submitted to microwave radiations, it is interesting to develop semianalytical solutions of the microwave absorbed power. Recently, a new approach based on asymptotes and resonances of microwave power proposed closed-form expressions for 1D propagation. Bhattacharya and Basak[17–19] developed a comprehensive analysis on microwave power absorption and show that the heat source pattern exhibits three distinct behaviors, which depend on two major length scales, that is, the wavelength and the penetration depth within the material.

Despite the usefulness of those 1D closed-form solutions, it is also necessary to obtain more complex models dedicated to microwave heating of 2D geometries.[2,20] Based on the closed-form solutions developed by Bhattacharya and Basak,[17,18] microwave heating of 2D sample submitted to nonuniform waves cannot be directly modeled. Because of the complexity of the 2D modeling, the coupling between the electromagnetic field and the heat equation is performed using a computational code, which solves numerically the Maxwell's equations. The COMSOL code has already been used successfully to model 2D microwave heating, and numerical results can be compared accurately to experimental measurements.[5]

Before extending the problem to 2D configurations, the first objective is to compare the closed-form expressions with 1D numerical simulation. Then, the second objective is to extend the validity of the closed-form expressions to 2D configurations with only the a priori knowledge of the incident electromagnetic field. A numerical procedure is applied to modify the sample thickness and to compare numerical and closed-form solutions for microwave power calculation.

Besides, from an industrial point of view, it is very interesting to know the efficiency of such a process. Therefore, the analysis of the reflected microwave power from the surface of the sample is also carried out.

Theoretical Aspects

Modeling of heat transfer during microwave heating

Heat transfer is based on the generalized heat equation, which depends on thermophysical properties of the product, as follows:

$$\rho C_p \frac{\partial T}{\partial t} = \mathrm{div}.(k\nabla T) + Q. \tag{1}$$

Into the general heat equation, Q denotes the heat source term and quantifies the amount of power which is dissipated within the product by dielectric losses.

To analyze the process of heat transport because of microwave heating, the following assumptions are introduced:

Assumption 1. The product receives the electromagnetic waves from the left surface.

Assumption 2. The product is surrounded by a medium with zero dielectric losses (air)

Assumption 3. The product is homogeneous and isotropic.

Assumption 4. The thermophysical and dielectric properties are constant.

Assumption 5. The mass transfer is negligible.

Assumption 6. Walls are perfectly insulated.

Assumption 7. The initial temperature T_0 of the sample is homogeneous.

Assumption 8. Heat transfers are not solved within air surrounding medium because of dielectric characteristics very close to vacuum.

Initial and Boundary Conditions. Convective coefficient $h = 2\ \mathrm{W\ m^{-2}\ K^{-1}}$ is due to natural convective flux at the left and right sides of the product.[18] The initial temperature is set to 300 K and the external temperature T_∞ within surrounding medium is equal to the same value.[18] Mathematically, the initial and boundary conditions can be written as:

$$\begin{cases} T = T_0 & \text{at } t = 0, \quad \forall x \forall z \\ k\dfrac{\partial T}{\partial z} = h(T - T_\infty) & \text{at } z = 0, \quad z = L, \forall x \\ k\dfrac{\partial T}{\partial z} = 0 & \text{at } x = 0, \quad x = a, \forall z \end{cases}. \tag{2}$$

Modeling of microwave propagation

Within dielectric mediums without free charges and free currents, the governing equations for a propagating electromagnetic wave in differential form are:

$$\begin{aligned} \nabla \times \boldsymbol{H} &= \frac{\partial \boldsymbol{D}}{\partial t} = \frac{\partial \varepsilon \boldsymbol{E}}{\partial t} \\ \nabla \times \boldsymbol{E} &= -\frac{\partial \boldsymbol{B}}{\partial t} = -\frac{\partial \mu \boldsymbol{H}}{\partial t} \\ \nabla.\boldsymbol{D} &= \nabla.\varepsilon \boldsymbol{E} = 0 \\ \nabla.\boldsymbol{B} &= \nabla.\mu \boldsymbol{H} = 0 \end{aligned} \tag{3}$$

ε is the complex permittivity and is defined as follows:

$$\varepsilon = \varepsilon_0 \varepsilon_\mathrm{r} = \varepsilon_0 \left(\varepsilon_\mathrm{r}' - j\varepsilon_\mathrm{r}''\right) \tag{4}$$

ε_r' is the dielectric constant and ε_r'' is the dielectric loss factor with $j^2 = -1$. For nonmagnetic materials, the permeability μ may be represented by $\mu_0 = 4\pi \times 10^{-7}\ \mathrm{H\ m^{-1}}$, the permeability of vacuum.[21]

In Eq. 3, Maxwell's equations relative to the electric field propagation can be transformed in sum of linear terms replacing derivative terms as a function of time. This form is particularly useful in engineering problems where electric and magnetic fields are time-variant fields following a harmonic law, with a pulsation $\omega = 2\pi f$, where f is the frequency of the wave.

As a consequence, the governing equation for electric field propagation is a Helmholtz equation depending only on space coordinates.

$$\nabla^2 \boldsymbol{E} + \omega^2 \mu_0 \varepsilon_0 \varepsilon_\mathrm{r} \boldsymbol{E} = 0. \tag{5}$$

1D Microwave Propagation. For 1D configuration problems, a semi-infinite slab is exposed to a uniform plane electromagnetic wave with normal incidence from the left surface (Figure 1).

The electric field within the dielectric sample has only one component E_y that varies along z direction. Equation 5 can be simplified to:

$$\frac{\partial^2 E_\mathrm{y}}{\partial z^2} + \omega^2 \mu_0 \varepsilon_0 \varepsilon_\mathrm{r} E_\mathrm{y} = 0. \tag{6}$$

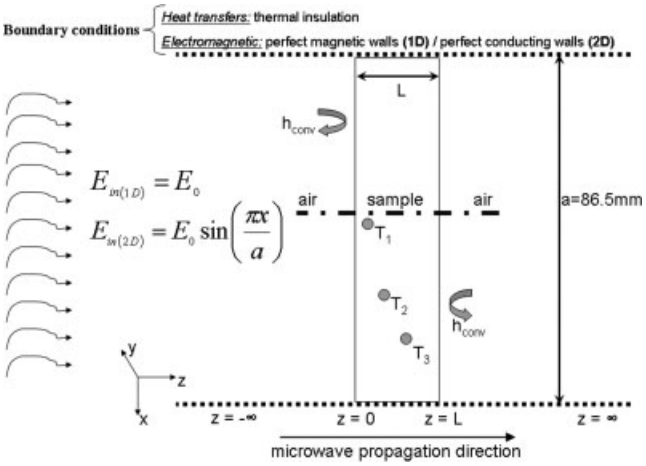

Figure 1. Model design for 1D and 2D configurations.

Initial and boundary conditions: Walls are perfect magnetic conductors to consider the propagation of a uniform plane electromagnetic wave within a semi-infinite media. The left surface of the sample is exposed to an incident electromagnetic wave. The microwave power flux at the left surface can be expressed from the power of the microwave generator and the surface area exposed to radiations ($S = ab$):

$$F_0(z = -\infty) = \frac{P_{\text{in}}}{ab}. \tag{7}$$

The amplitude of the incident electric field is calculated in air surrounding medium. The relation between the incident microwave power and the amplitude of the electric field is[22]:

$$E_{\text{in}}(z = -\infty) = E_0 = \sqrt{\frac{4Z_0P_{\text{in}}}{ab}}. \tag{8}$$

In free space, the wave impedance Z_0 is calculated as follows[23]:

$$Z_0 = \sqrt{\frac{\mu_0}{\varepsilon_0}}. \tag{9}$$

The wave impedance within the dielectric sample is[23]:

$$Z_{\text{sample}} = \sqrt{\frac{\mu_0}{\varepsilon_0\varepsilon_{\text{r}}'}}. \tag{10}$$

The electric field propagation within the air is governed by the propagation constant.

$$\kappa_{\text{air}} = \sqrt{4\pi^2\varepsilon_0\mu_0 f}, \tag{11}$$

where f is the frequency of the microwave radiations. For the particular case of 1D propagation within semi-infinite media, the cutoff frequency is zero.

The reflection factor between an incident electromagnetic wave and a dielectric sample is defined as[24]:

$$RF = \frac{P_{\text{reflected}}}{P_{\text{in}}}. \tag{12}$$

The incident electromagnetic wave is uniform along x axis (1D propagation). To our knowledge, no appropriate relationships are available in the literature to determine the wave reflection factor as a function of sample lengths and dielectric properties.

Thus, the wave reflection factor between the air and the sample is computed from the numerical resolution of Maxwell's equations. The reflection factor is obtained by numerical integrations of the reflected power at left side with respect to the incident power coming from the microwave generator.

$$\text{RF} = \left(\frac{\int\limits_{\text{port}} \left((\boldsymbol{E}_{\text{c}} - \boldsymbol{E}_1).\boldsymbol{E}_1^* \right) dS}{\int\limits_{\text{port}} \left(\boldsymbol{E}_1.\boldsymbol{E}_1^* \right) dS} \right)^2, \tag{13}$$

where E_{c} is the computed electric field on the excitation port at left side ($z = -\infty$). E_{c} represents the total electric field (excitation plus the reflected field) and E_1 is the electric field pattern on excitation port.

Under certain operating conditions, classical relations are available in the literature to determine the reflection factor between the air and a dielectric medium.[22,23,25,26] These relations are limited to uniform plane electromagnetic waves within semi-infinite mediums sufficiently thick and surrounded by zero dielectric losses.[25]

$$\text{RF} = 1 - \frac{16\pi^2}{\lambda_0\lambda_{\text{m}}\left(4\pi^2\left(\frac{1}{\lambda_0} + \frac{1}{\lambda_{\text{m}}}\right)^2 + \frac{1}{D_{\text{p}}^2}\right)}. \tag{14}$$

In Eq. 14, λ_0 is the wavelength in free space and λ_{m} is the wavelength within the dielectric medium, which depends on dielectric properties.[18]

$$\lambda_0 = \frac{C_0}{f} \tag{15}$$

$$\lambda_{\text{m}} = \frac{C_0\sqrt{2}}{f\left[\sqrt{\varepsilon_{\text{r}}'^2 + \varepsilon_{\text{r}}''^2} + \varepsilon_{\text{r}}'\right]^{1/2}}. \tag{16}$$

Microwave penetration depth relative to the electric field is the distance at which the electric field strength decays of $1/e$ of its original value at the surface. Mathematically, the electric field penetration depth depends on dielectric properties of the product.[27]

$$D_{\text{p}} = \frac{C_0}{\sqrt{2}\pi f\left[\sqrt{\varepsilon_{\text{r}}'^2 + \varepsilon_{\text{r}}''^2} - \varepsilon_{\text{r}}'\right]^{1/2}}. \tag{17}$$

If $\varepsilon'' \ll \varepsilon'$, Eq. 14 can be simplified and the reflection factor reduces to the following equation by only taking into account dielectric properties values[26]:

$$\text{RF} = \left(\frac{\sqrt{\varepsilon_{\text{r}}'} - 1}{\sqrt{\varepsilon_{\text{r}}'} + 1} \right)^2. \tag{18}$$

At the interface between air surrounding medium and the dielectric sample ($z = 0$ and $z = L$), the electric field is continuous.

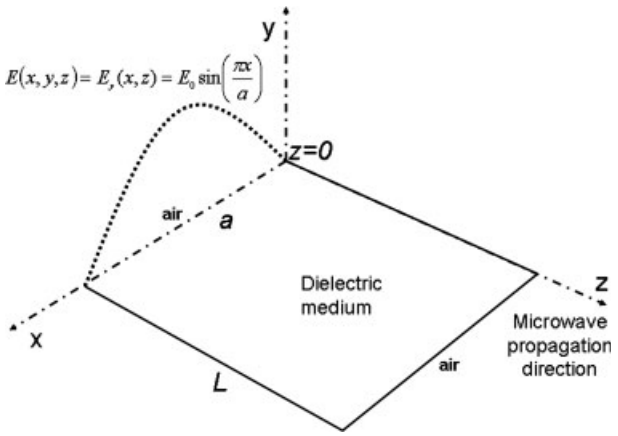

Figure 2. Schematic representation of microwave propagation within 2D rectangular waveguide.

At the right side of the sample ($z = L$), the resulting electromagnetic wave propagates without any reflection.

Mathematically, initial and boundary conditions can be written as:

$$\begin{cases} E = 0 & \text{at } t = 0, \quad \forall x\, y\, z \\ E_{\text{in}} = E_0 & \text{at } z = -\infty, \quad \forall x \\ n \times \left(\boldsymbol{H}_{\text{air}} - \boldsymbol{H}_{\text{sample}}\right) = 0 & \text{at } z = 0,\ z = L, \quad \forall x \\ n \times \boldsymbol{H} = 0 & \text{at } x = 0,\ x = a, \quad \forall z \end{cases} \tag{19}$$

Microwave Propagation Within 2D Rectangular Waveguide. Assuming microwave propagation in TE_{10} fundamental mode, the incident electric field is nonuniform within the (xOy) plane (Figure 2).

For microwave propagation in z direction, the development of Eq. 5 shows that the electric field distribution does not depend on y coordinates regarding the shape of the incident electric field. Thus, the electric field is contained within the (xOy) plane with only one component E_y.

Equation 5 can be written as follows:

$$\left(\frac{\partial^2 E_y}{\partial x^2} + \frac{\partial^2 E_y}{\partial y^2} + \frac{\partial^2 E_y}{\partial z^2}\right) + \omega^2 \mu_0 \varepsilon_0 \varepsilon_r E_y = 0. \tag{20}$$

In the transversal plane (xOy), a plane electromagnetic wave is considered with no variations along y direction. As a result, $\partial^2 E_y/\partial y^2 = 0$.

The term $\partial^2 E_y/\partial x^2$ represents the variations of the electric field strength along the large edge of the rectangular waveguide. The incident electric field is a parametric function along x direction and microwave propagation occurs along z direction. Thus, Eq. 20 can be simplified as follows:

$$\left(\frac{\partial^2 E_y}{\partial x^2} + \frac{\partial^2 E_y}{\partial z^2}\right) + \omega^2 \mu_0 \varepsilon_0 \varepsilon_r E_y = 0. \tag{21}$$

Initial and boundary conditions: Walls of the waveguide are perfect electric conductors. The left surface of the sample is exposed to an incident electromagnetic wave.

In TE_{10} mode, considering a rectangular guide filled by a homogeneous dielectric sample, the incident electric field is straightforwardly obtained from the resolution of Maxwell's equations. The microwave incident power flux can be expressed from the power of the microwave generator. For a sinusoidal wave in TE_{10} mode, the microwave power flux is calculated using the following expression[28]:

$$F_0(x, z = -\infty) = \frac{P_{\text{in}}}{\text{ab}} \sin^2\left(\frac{\pi x}{a}\right). \tag{22}$$

The amplitude of the incident electric field along x axis is calculated in air surrounding medium using the following relation:

$$E_{\text{in}}(x, z = -\infty) = E_0 \sin\left(\frac{\pi x}{a}\right) = \sqrt{\frac{4 Z_{\text{TE}\,0} P_{\text{in}}}{ab}} \sin\left(\frac{\pi x}{a}\right). \tag{23}$$

Within a rectangular wave guide in fundamental TE_{10} mode, $Z_{\text{TE}\,0}$ is the wave impedance in air surrounding medium[14,29]:

$$Z_{\text{TE}\,0} = \frac{\lambda_{g0}}{\lambda_0} \sqrt{\frac{\mu_0}{\varepsilon_0}}, \tag{24}$$

where λ_{g0} is the wavelength within the rectangular waveguide[30]:

$$\lambda_{g0} = \frac{\lambda_0}{\sqrt{1 - \left(\frac{\lambda_0}{\lambda_c}\right)^2}}. \tag{25}$$

In the typical case of the fundamental TE_{10} mode, the cutoff wavelength λ_c is $2a$. In TE_{10} mode, at 2.45×10^9 Hz, the cutoff frequency is 1.73×10^9 Hz. This leads to the following propagation constant in air surrounding medium.

$$\kappa_{\text{air}} = \sqrt{4\pi^2 \varepsilon_0 \mu_0 (f - f_c)}. \tag{26}$$

The incident electromagnetic wave is nonuniform along x axis. As a result, wave reflection between the air and the surface of the product cannot be calculated using analytical expressions for semi-infinite slabs.[25] To avoid this difficulty, the wave reflection factor between the air and the sample is determined from the numerical resolution of Maxwell's equations (Eq. 13).

In our case, the incidence of the microwave signal is normal to the left side of the sample. For sufficiently thick samples, a general relationship allows computing the wave reflection factor between two mediums of different permittivity.[23,24]

$$\text{RF} = \left(\frac{Z_{\text{TE sample}} - Z_{\text{TE}\,0}}{Z_{\text{TE sample}} + Z_{\text{TE}\,0}}\right)^2 \tag{27}$$

For a waveguide configuration, the wave impedance Z is calculated in both air and dielectric medium. By analogy with Eq. 24, the wave impedance within the dielectric sample is calculated as follows:

$$Z_{\text{TE sample}} = \frac{\lambda_{g\,\text{sample}}}{\lambda_m} \sqrt{\frac{\mu_0}{\varepsilon_0 \varepsilon_r}}, \tag{28}$$

where the guided wavelength λ_g within the sample is calculated by replacing λ_0 by λ_m in Eq. 24.

At the end of the rectangular waveguide, the resulting electromagnetic wave exits the guide without any reflection.

Mathematically, the initial and boundary conditions can be written as:

$$\begin{cases} E = 0 & \text{at } t = 0, \quad \forall xyz \\ E_{\text{in}} = E_0 \sin\left(\dfrac{\pi x}{a}\right) & \text{at } z = -\infty, \quad \forall x \\ n \times \left(\boldsymbol{H}_{\text{air}} - \boldsymbol{H}_{\text{sample}}\right) = 0 & \text{at } z = 0, z = L, \quad \forall x \\ E_{\text{yt}} = 0 & \text{at } x = 0, x = a, \quad \forall z \end{cases} \quad . \tag{29}$$

Microwave power calculation

From Maxwell's Equations. The Poynting vector is used to quantify the amount of power dissipated by dielectric losses within a medium. This vector represents the energy carried by the electromagnetic wave.

$$P(t) = \boldsymbol{E}(t) \times \boldsymbol{H}(t) \tag{30}$$

From the Poynting vector, the absorbed power by unit volume can be calculated from the local electric field strength[17,31,32]:

$$Q = \frac{1}{2}\omega\varepsilon_0\varepsilon''\boldsymbol{E}^2. \tag{31}$$

The resolution of Maxwell's equations leads to the local electric field amplitude within the computational domain and it allows calculating the heat generation term because of microwaves.

From Closed-Form Expressions. Equation 31 clearly shows the strong dependence of the absorbed power on the electric field strength within the sample.[17,18]

Microwave propagation equations in air surrounding medium and dielectric sample can be written as a linear combination of transmitted and reflected waves propagating in opposite directions.[18]

$$\begin{array}{ll} E_{\text{y,air}} = E_{\text{t,air}}e^{j\kappa_{\text{air}}z} + E_{\text{r,air}}e^{-j\kappa_{\text{air}}z} & z \in \{-\infty, 0\} \\ E_{\text{y,sample}} = E_{\text{t,sample}}e^{j\kappa_{\text{sample}}z} + E_{\text{r,sample}}e^{-j\kappa_{\text{sample}}z} & z \in \{0, L\} \\ E_{\text{y,air}} = E_{\text{t,air}}e^{j\kappa_{\text{air}}z} + E_{\text{r,air}}e^{-j\kappa_{\text{air}}z} & z \in \{L, \infty\} \end{array}, \tag{32}$$

where E_{t} and E_{r} are the coefficients of transmission and reflection, respectively.

Closed-form relationships were developed by Bhattacharya and Basak,[17,18] and the resulting expressions lead to the absorbed power distribution within the sample.

Within the following mathematical development, microwave left side incidence is only considered and the closed-form relationships are based on the following assumptions:

- The initial work from Bhattacharya and Basak[17,18] is valid for a semi-infinite slab of length L exposed to uniform plane microwave radiations with normal incidence at the left side (Figure 1).
- Dielectric properties are constant on the working temperature range.
- The surrounding medium at left and right sides of the product is considered to have zero dielectric loss. This statement is true if the free space is occupied by air whose dielectric properties are very close to vacuum.

The closed-form expressions are useful to predict the heat source term as it can be directly obtained from the incident electric field at left side of the sample. The closed-form solutions developed by Bhattacharya and Basak are based on two length scales, which govern the microwave power formulation. Namely, the two governing parameters are the sample length and the penetration depth of microwaves within the sample.

z' is defined as a dimensionless coordinate, normalized by half thickness of the sample.

$$z' = \frac{2z}{L} \tag{33}$$

The relationship that links the penetration depth to the wavelength within the dielectric medium leads to the propagation constant within the sample.[17]

$$\kappa_i = \kappa_{ia} + j\kappa_{ib} = \frac{2\pi}{\lambda_i} + j\frac{1}{(D_{\text{p}})_i} \tag{34}$$

The general expression, $\kappa_i = \kappa_{ia} + j\kappa_{ib}$ defines the propagation constant into i medium.

- $i = 1$ for surrounding medium at left side (air)
- $i = 2$ for dielectric medium (sample)
- $i = 3$ for surrounding medium at right side (air).

Microwave power exhibits three distinct regimes depending on the relative magnitude of the two previous lengths scale.

- If $L \gg D_{\text{p}}$, the absorbed power within the sample is governed by a decreasing exponential law from left to right side of the product («thick sample asymptote» or «Lambert' law»). For a left side incidence, the microwave absorbed power within the sample is calculated from the following expression[18]:

$$Q = 4\pi f\varepsilon_0\varepsilon_2'' \frac{|\kappa_1|^2 e^{(\kappa_{1b}-\kappa_{2b})L} e^{-\kappa_{2b}Lz'} E_{\text{in}}^2}{|\kappa_1|^2 + |\kappa_2|^2 + 2\delta_{12}^R} \tag{35}$$

- If $0 < L \ll l_{\min}$, with $l_{\min} \equiv \min\left(\frac{\lambda_{\text{m}}}{2\pi}, D_{\text{p}}\right)$, hence microwave absorbed power is uniform into the sample («thin sample asymptote»). This regime is valid for very thin samples and no more mathematical details will be given in this article.
- If $D_{\text{p}} \gg L \gg l_{\min}$, the power profile depends on the ratio of the penetration depth and the wavelength within the dielectric medium. The regime is called resonant and microwave absorbed power exhibits minima and maxima at different locations of the product along the propagation direction. The microwave absorbed power is calculated from the following relationship[17]:

$$Q = \frac{8\pi f\varepsilon_2''\kappa_0^2}{C_0} \times \frac{C^-}{C^{\text{d}}} \times F_0 \tag{36}$$

The closed-form solutions are obtained from Maxwell's equations.[2,18] From the closed-form expressions, the incident electric field at left side is the only needed variable to compute the heat source term within the sample. In this case, the wave reflection factor between air surrounding medium and the product does not need to be calculated.

Table 1. Thermophysical and Dielectric Properties for Oil and Water[25]

	Oil	Water
Density, ρ (kg m^{-3})	900	1000
Specific heat, C_p (J kg^{-1} K^{-1})	2000	4190
Thermal conductivity, k (W m^{-1} K^{-1})	0.168	0.609
Dielectric constant, ε_r' (2450 MHz)	2	79.5
Dielectric loss factor, ε_r'' (2450 MHz)	0.15	9.6
Electric field penetration depth, D_p (cm)	36.8	3.6
Wavelength within sample, λ_m (cm)	8.64	1.37

The purpose of this study is to extend those solutions to 2D configuration problems where the incident electric field is nonuniform along the large edge of a rectangular waveguide in fundamental TE_{10} mode.

Materials and Methods

The computational scheme

For 1D configuration problems, closed-form relationships and numerical results are tested to determine the microwave absorbed power. First, 1D's numerical simulations are performed using Maxwell's equations approach. Numerical solutions are obtained using a finite element code, COMSOL®3.3. Numerical results are compared with closed-form relationships dedicated to microwave power[17,18] to validate the simulations for semi-infinite slabs.

Then, the study is extended to a 2D configuration problem where the incident electric field is nonuniform along the left side of the sample (TE_{10} fundamental mode). The 2D simulation results were previously validated with experimental measurements during 2D microwave heating in rectangular waveguide.[5] Numerical results are compared with the closed-form expressions by taking into account the nonuniformity of the incident electric field along the left side of the sample. Thus, for the 2D modeling, mathematical expressions of the initial closed-form solutions[17,18] are not modified. The 2D semianalytical model can be represented as multiple wave propagations along z direction with a parametric function of incident electric field along x direction (Figure 2).

Low and high dielectrics are chosen as testing materials during calculations, respectively, oil and water. Each of those two dielectric materials illustrates extreme cases with products having, respectively, low and high dielectric properties. Table 1 presents thermophysical and dielectric properties values for the two tested materials. Data for oil and water are taken from Barringer et al.[25]

For both 1D and 2D configurations, a parametric study is performed using the numerical simulation and the closed-form expressions. An original numerical procedure is used to modify both numbers of mesh elements and sample lengths at each computational step. This procedure allows evaluating the geometrical impact on the absorbed power profile within the sample.

First, initial parameters such as temperature, microwave input power, and sample length are fixed. Then, simulations are performed separately by choosing each of the two dielectric materials, that is, oil or water associated with their dielectric properties. Microwave absorbed power is computed using both approaches, that is, numerical vs. closed-form expressions for 1D and 2D configurations. At each computational step, initial sample length is increased by 1 mm. The computation lasts until the sample length reaches 103 mm, which is a compromise between accuracy and memory requirement. The computational scheme is detailed in Figure 3.

The 1D and 2D numerical approaches consist in solving the Maxwell's equations using COMSOL®, release 3.3, (Radio Frequency module). COMSOL® uses Galerkin finite element method as numerical technique to solve problems described by systems of partial differential equations. The geometry consists of one rectangular sample surrounded by two air layers located at left and right sides of the sample, respectively. Regarding the simplicity of the geometry, the quadrangle element was used as the basic element type for the mesh. The grid independence of numerical results is determined by using a quality criterion for the mesh. This criterion is based on aspect ratio, which means that anisotropic elements can get a low quality measure even though the element shape is reasonable. For a quadrangle element, the element quality of a quadrilateral is defined as follows:

$$q = \frac{4A}{l_1^2 + l_2^2 + l_3^2 + l_4^2} \tag{37}$$

where A is the surface of the quadrilateral and l_1–l_4 are the side lengths. The value of q is a number between 0 and 1, which depends on the element quality. Note that for a square the best element quality is 1.

Numerical tests were performed to obtain the mesh independence and, in our case, results reveal that the minimum element quality is $q_{min} = 0.87$. This value is a good

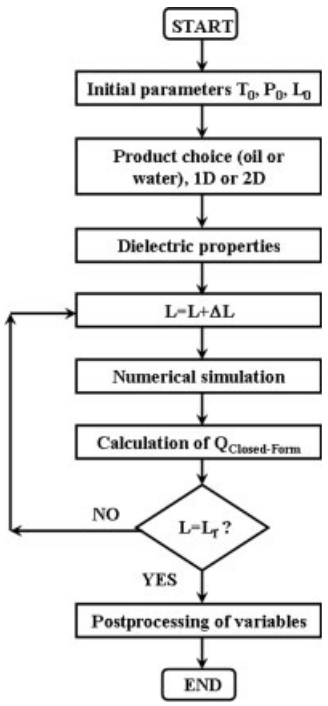

Figure 3. Computational scheme.

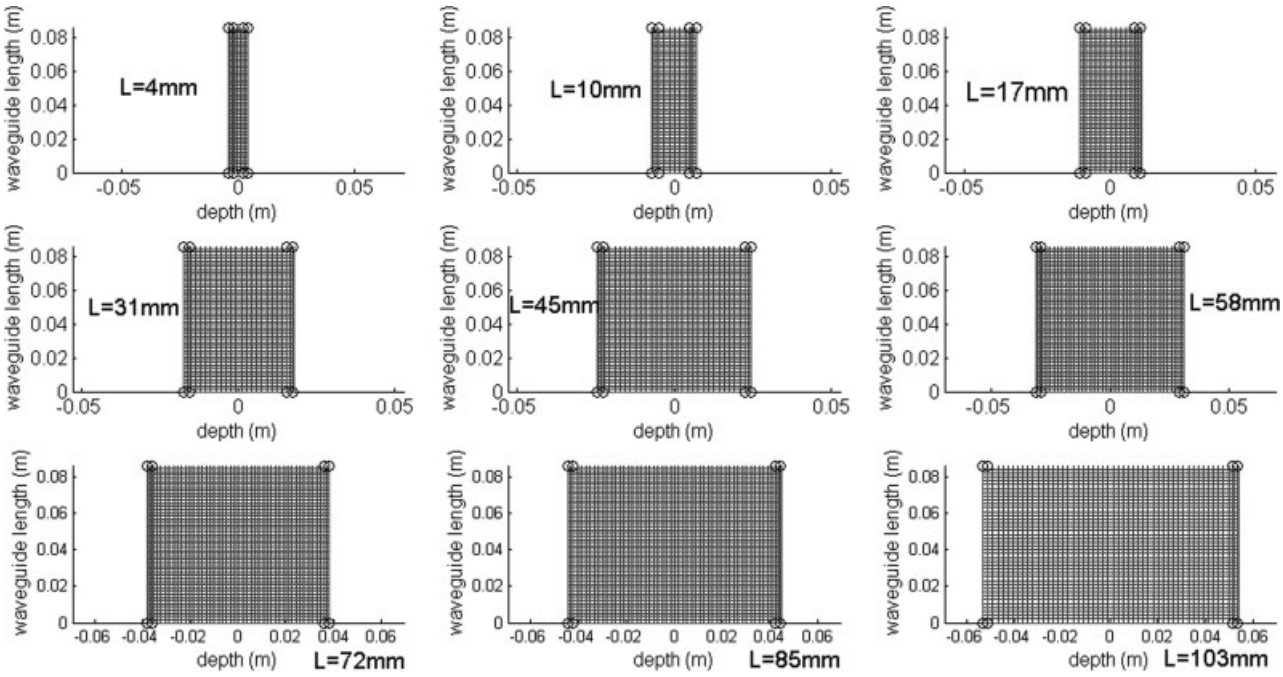

Figure 4. Example of mesh adaptation as a function of sample length.

compromise between accuracy and computational time during numerical simulations. Hence, the mesh is adapted to the sample size by respecting the minimum element quality (Figure 4). The number of quadrangle elements within air surrounding medium does not influence the numerical results. To reduce the computational times, the air layer is modeled with the finest thickness.

The 1D and 2D problems with the closed-form expressions are solved analytically by using the mathematical expressions depending on the microwave power regime (resonant or exponential).

Results and Discussions

Microwave absorbed power

The first part of the study compares closed-form expressions and numerical simulations for a semi-infinite slab (1D configuration). Then, closed-form relationships are extended to a 2D waveguide configuration where the electric field is nonuniform along the left side of the sample (TE_{10} mode). Two-dimensional semianalytical results obtained from closed-form expressions are compared with 2D numerical simulations to see if whether or not results are different. For all calculations, the input parameters are fixed to the following values:

$$\frac{P_{\text{in}}}{ab} = 3 \times 10^4 \text{W/m}^2$$
$$L_0 = 4\,\text{mm} \quad \Delta L = 1\,\text{mm} \quad L_{\text{f}} = 103\,\text{mm}$$

Results for Water Sample. Microwave penetration depth for water equals 36.3 mm according to Eq. 17. Water behaves like a high dielectric material regarding its dielectric properties values. Thus, there is a strong interaction between the electromagnetic wave and the sample. According to Bhattacharya and Basak,[18] the resonating regime is predominant for sample length ranging from $l_{\text{min}} = 2 \times 10^{-3}$ m to $D_{\text{p}} = 0.036$ m. The Lambert's exponential decay law is valid for sample length much bigger than $D_{\text{p}} = 0.036$ m.

1D configuration: In Figure 5, the numerical simulation allows computing the wave reflection factor between the air and the sample for sample length ranging from 4 to 103 mm.

In resonating regime, the reflection factor is characterized by huge variations as sample length increases. For 4-mm sample depth, almost 90% of the microwave input power is reflected at the interface between the air and the sample. On the contrary, for 7-mm-depth sample, reflection factor is

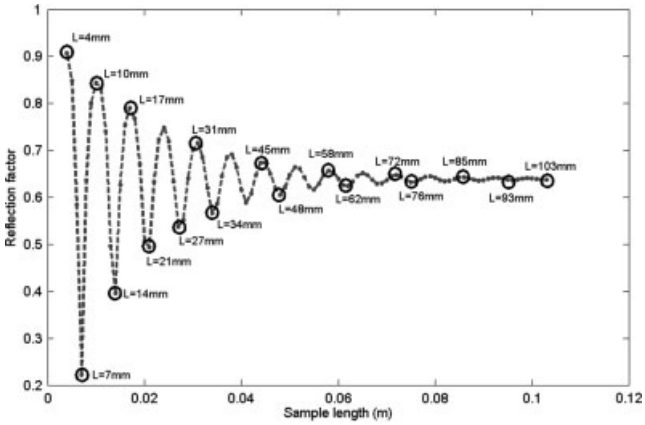

Figure 5. Reflection factor from 1D numerical simulation as a function of sample length for water.

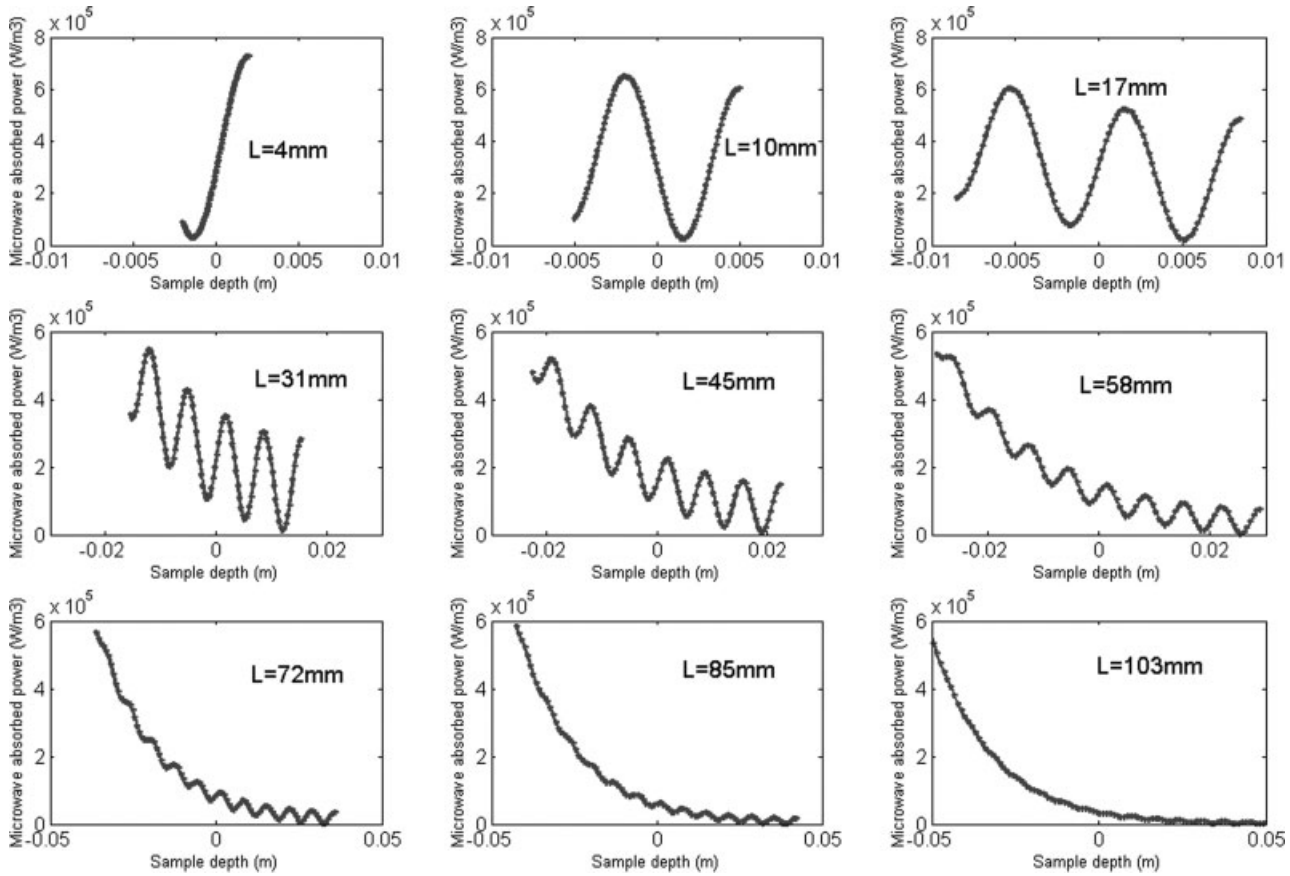

Figure 6. Microwave absorbed power for water (1D), high reflection factors, – numerical simulation -- closed-form expressions from Bhattacharya and Basak.[17,18]

only 22%. The heating rate is therefore enhanced for 7-mm compared with 4-mm sample length.

In resonating regime, the numerical simulation shows that reflection factor does not only depend on dielectric properties but also on sample length. The variations are more and more attenuated as sample length increases.

The global variation of the reflection factor is characterized by a damping wave, which tends to stabilize as sample length increases. For a sample length bigger than 85 mm, the reflection factor reaches an asymptote.

Let us consider a water sample sufficiently thick to avoid the effect of multiple wave reflections within the product (thick sample regime). For a uniform plane electromagnetic wave with normal incidence, the reflection factor at air–water interface is 63% (Eq. 14). This value is confirmed with 1D numerical simulation when the reflection factor value reaches a constant.

Figures 6 and 7 display the microwave absorbed power within water sample along the propagation direction z of microwaves. Microwave incidence occurs at left side of the sample. Specific sample lengths are chosen as a function of picks and valleys of reflection factors (Figure 5). Numerical results (Eq. 31) are compared with the closed-form expressions (Eqs. 35 and 36).

Figures 6 and 7 clearly show that the closed-form expressions fit well to 1D numerical simulation. Both amplitude and phase between each sinusoid are exactly the same. Therefore, 1D numerical simulation is validated with the closed-form expressions dedicated to microwave power calculation.

For sample length ranging from 4 to 85 mm, the resonating regime is well characterized and an oscillating behavior of microwave power can be observed within the sample.

For 4-mm sample length, the microwave heating rate is higher at the right side compared with the left side of the sample. Hence, this phenomenon confirms that sample size plays an important role in the microwave heating process.[18,25] When sample size increases from 4 to 7 mm, the maximum absorbed power rises from $\sim 7 \times 10^5$ to 4×10^6 W m^{-3}.

In a thermal point of view, minima and maxima of microwave power lead to cold and hot spots within the product. These heterogeneous heating patterns are characterized by local microwave power concentrations along the propagation direction.

For 31-mm depth, five hot spots are noticed regarding picks of microwave absorbed power within the sample. The number of heating patterns rises as sample length increases.

For a sample depth bigger than 70 mm, the resonating regime tends to disappear to the benefit of an exponential decreasing function. According to the previous theoretical part, the microwave absorbed power follows the Lambert's

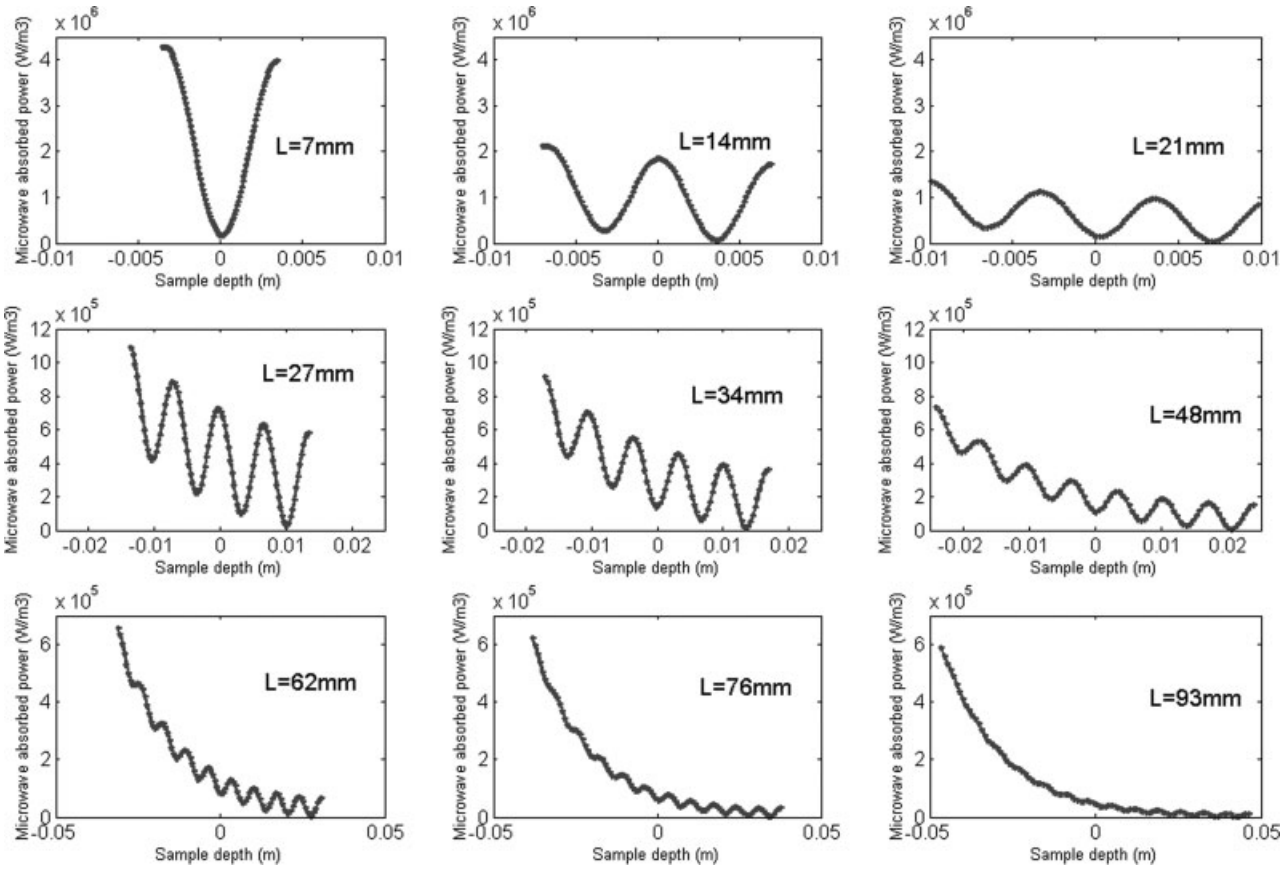

Figure 7. Microwave absorbed power for water (1D), low reflection factors, – numerical simulation -- closed-form expressions from Bhattacharya and Basak.[17,18]

law behavior if sample length is much bigger than the penetration depth value. For 103-mm-thick sample, the sample length is approximately three times the penetration depth value and the resonating behavior of microwave power may be neglected. According to Lambert's law (thick sample regime), microwave power concentration is located near the left surface of the product without any resonating behavior along the propagation direction.

2D configuration: In Figure 8, the 2D numerical simulation allows computing the wave reflection factors between the air and the sample for sample lengths ranging from 4 to 103 mm. Although the global profile of the reflection factor is the same as for 1D simulation, some amplitude differences are noticed. According to 2D numerical results, the reflection factors for the tested sample lengths are $\sim$10% higher than for 1D simulation. The lowest reflection factors are obtained for 7 and 14 mm sample length, respectively, 32 and 50%.

Within a waveguide structure, the reflection factor between air and water for a thick sample regime is 73% (Eq. 27). This reflection factor value is confirmed with the numerical simulation for sample length bigger than 85 mm (Figure 8).

Figures 9 and 10 display microwave absorbed power along a cross section line located at the center of the water sample. Microwave incidence occurs at the left side of the sample and the input surface power is max at the center (TE_{10} mode). The tested sample lengths are chosen from 1D simulation.

On the whole, Figures 9 and 10 show that the closed-form expressions fit well to the 2D numerical simulations. The phase between each sinusoid is well respected for all sample lengths; however, some amplitude differences are noticed between both approaches, especially for 7- and 14-mm sample lengths. Those particular lengths correspond to the lowest reflection factors, 32 and 50%, respectively. Hence, the

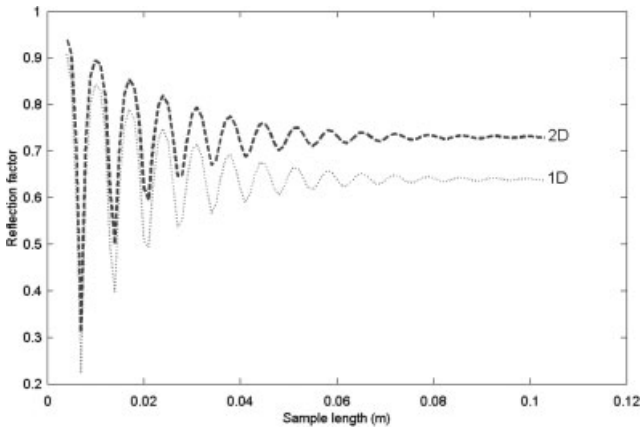

Figure 8. Reflection factor from 1D and 2D numerical simulation as a function of sample length for water—$l_{min} = 2 \times 10^{-3}$ m, $D_p = 0.036$ m.

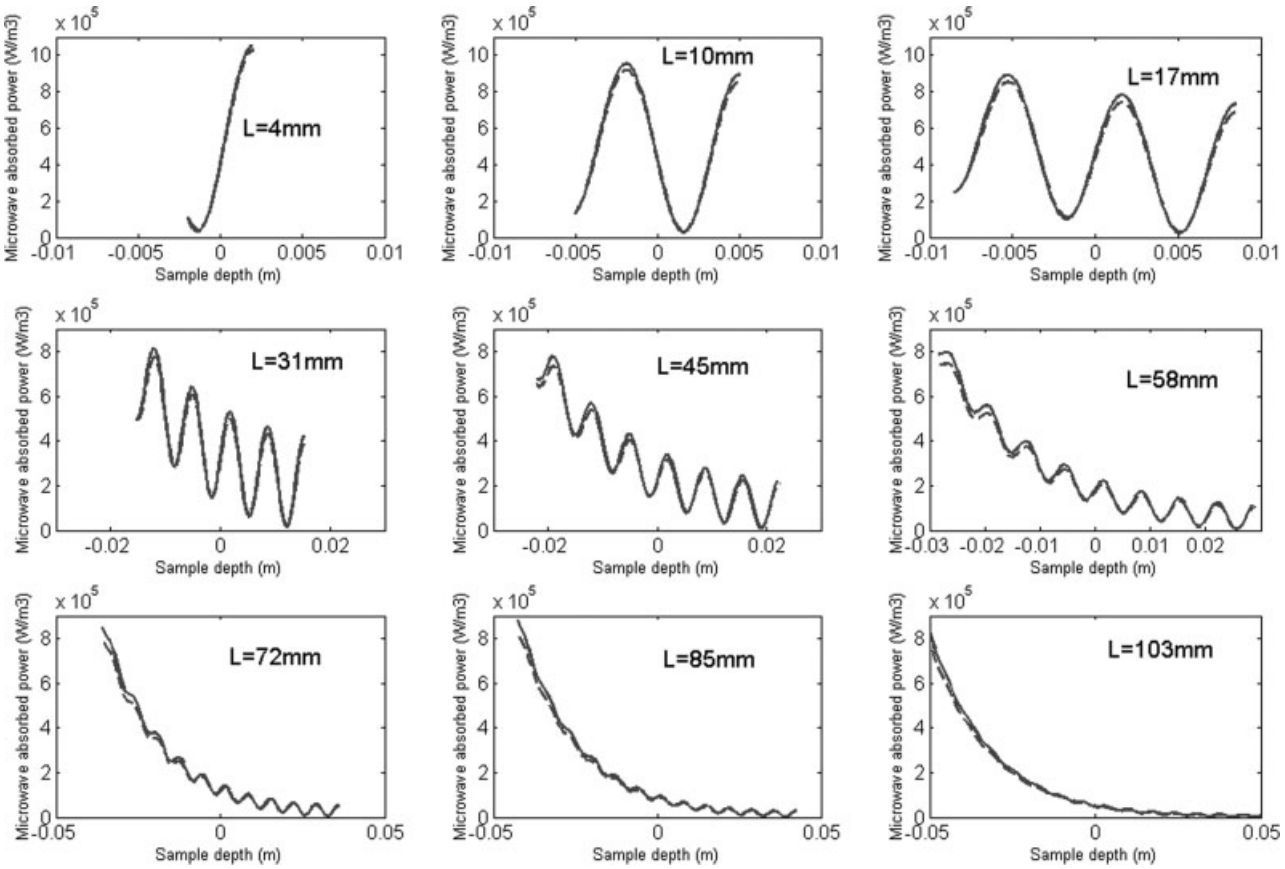

Figure 9. Microwave absorbed power for water (2D), high reflection factors, – numerical simulation -- closed-form expressions from Bhattacharya and Basak.[17,18]

absorbed power computed from the 2D numerical simulation is slightly higher than the one calculated from the closed-form expressions. These variations can explain the amplitude differences between both approaches for 7- and 14-mm sample depths.

For all other sample lengths, the influence of the reflection factor as a function of sample length is negligible. This leads to a good correlation between both approaches within a 2D rectangular waveguide.

The closed-form expressions are a reliable tool to predict microwave absorbed power within high dielectric materials. For 1D configuration and various sample lengths, both numerical and closed-form expressions give very similar results in resonating regime and ''thick sample regime.'' However, for 2D configurations, small discrepancies are observed between both approaches at specific sample lengths. Those differences are attributed to reflection factor variations as a function of sample length. On the whole, good agreement is found between both approaches in 2D configuration for water sample.

Results for Oil Sample. Microwave penetration depth for oil sample is 367.7 mm (Eq. 17). This value is $\sim$10 times the penetration depth for water sample. According to Bhattacharya and Basak, the resonating regime is predominant for sample length ranging from $l_{\min} = 0.0138$ m to $D_p = 0.368$ m. The Lambert's exponential decay law is valid for sample lengths much bigger than $D_p = 0.368$ m.

Figure 11 displays microwave absorbed power within oil sample for a 1D microwave propagation. Only three specific sample lengths are chosen to characterize the oscillating behavior of microwave power within resonating regime.

Figure 11 clearly shows that the closed-form expressions for microwave power fit well to the 1D numerical simulation as explained with high dielectric loss sample. Both amplitude and phase between each sinusoid are exactly the same for the two approaches.

Figure 12 displays microwave absorbed power within oil sample for a 2D microwave propagation. For each sample length and both approaches, the absorbed power does not correspond. The global shape of the curves is quite close but amplitude variations and phase shifts are noticed.

In Figure 13, the reflection factor between the air and the oil sample is computed using 1D and 2D numerical simulations for sample lengths ranging from 4 to 103 mm.

Approximately, 0–20% of the microwave input power is reflected from the surface of oil sample. Variations are relatively small compared with previous values for the water sample. In this case, the dielectric medium is more transparent to microwaves and most of the microwave power is transmitted through the product.

Reflection factor amplitudes are lower for 1D simulations compared with 2D simulations. The same observations were noticed for water sample, but a phase shift is also noticed for oil sample.

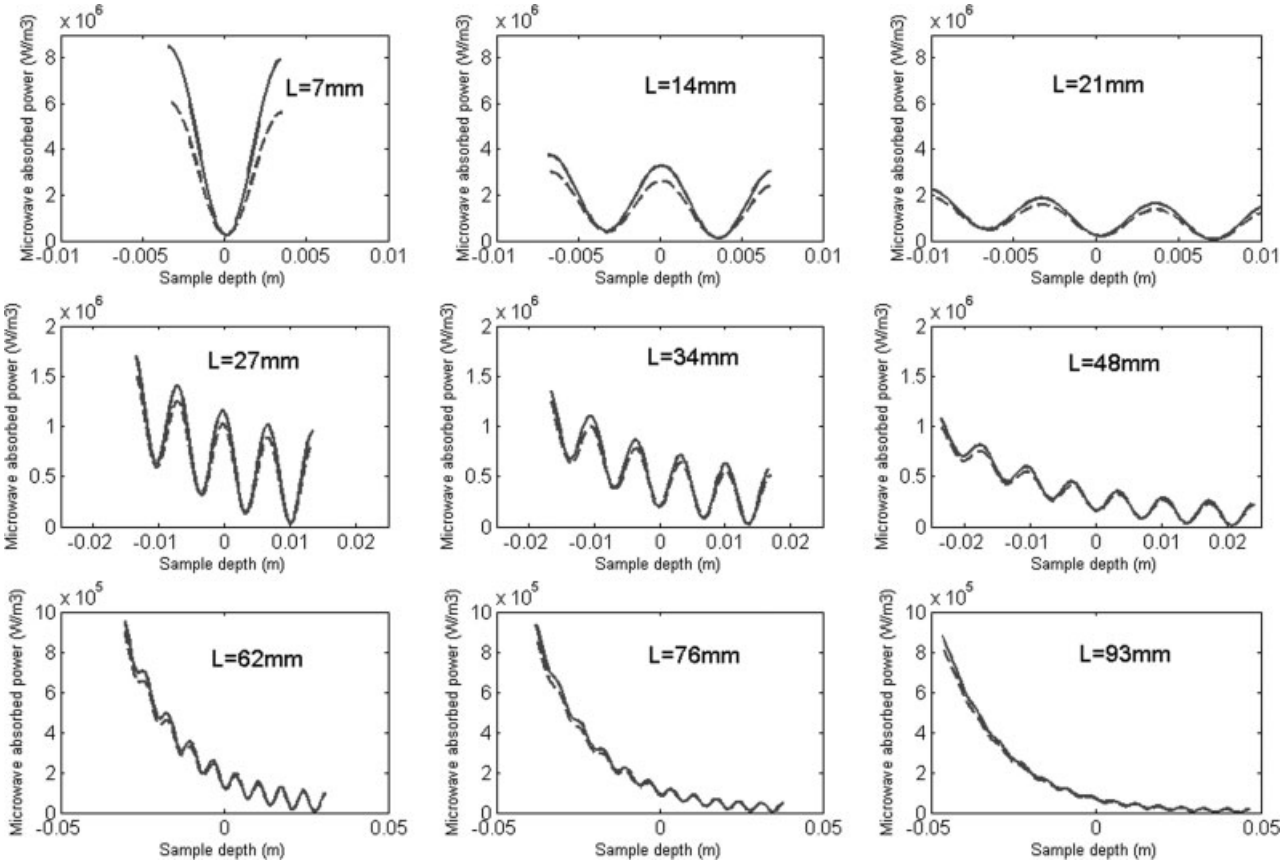

Figure 10. Microwave absorbed power for water (2D), low reflection factors, – numerical simulation -- closed-form expressions from Bhattacharya and Basak.[17,18]

The global shape of the reflection factor shows a wavy behavior as a function of sample length. The amplitude of the wave tends to decrease as sample length increases. This leads to a smaller damping of the reflection factor compared with the results for water sample. For a sample length much bigger than the penetration depth, the reflection factor is supposed to reach an asymptote. For oil sample, this value is predictable. In thick sample regime and for a uniform plane wave with normal incidence (1D), this asymptote is equal to 3% (Eq. 14). For microwave propagation in guided structures (2D), the reflection factor at air–oil interface is 7% (Eq. 27).

Comparison Between 2D Numerical Results. In 2D configuration, the incident electromagnetic wave is nonuniform along the left surface of the sample. The wave propagation equation depends on both x and z coordinates according to Eq. 21:

$$\left(\frac{\partial^2 E_y}{\partial x^2}+\frac{\partial^2 E_y}{\partial z^2}\right)+\omega^2\mu_0\varepsilon_0\varepsilon_r E_y=0$$

The second derivative of electric field $\partial^2 E_y/\partial z^2$ represents variations of the electric field along the propagation direction z, whereas $\partial^2 E_y/\partial x^2$ quantifies electric field variations along x direction.

In Figure 14, the second derivatives of the electric field ($\partial^2 E_y/\partial x^2$ and $\partial^2 E_y/\partial z^2$) are plotted on a cross section line located at the center of the sample along the propagation

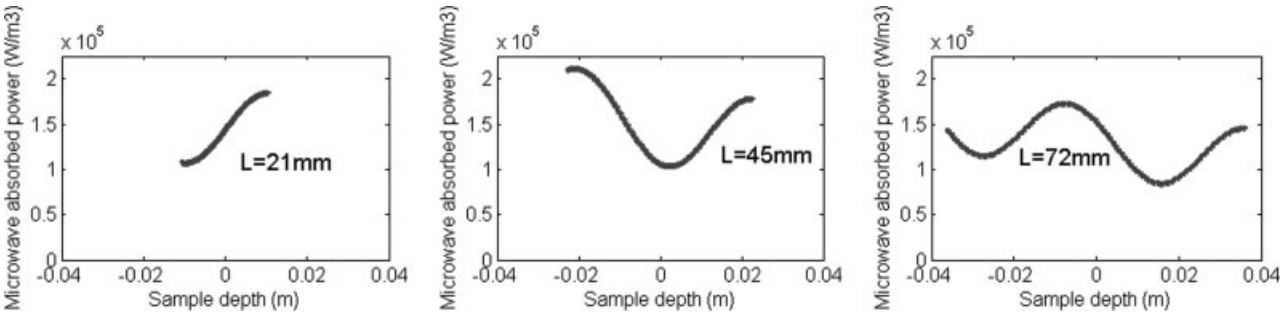

Figure 11. Microwave absorbed power for oil (1D), – numerical simulation ---closed-form expressions.[17,18]

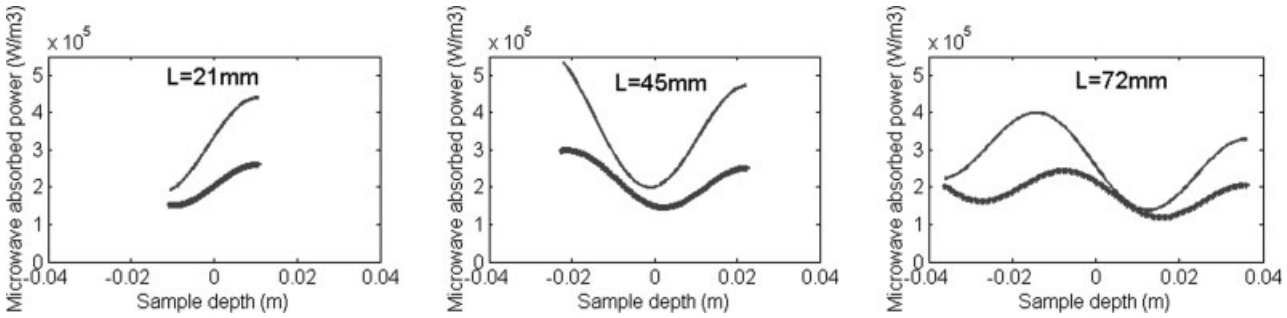

Figure 12. Microwave absorbed power for oil (2D), – numerical simulation -- closed-form expressions.[17,18]

direction z. For both oil and water, the figures illustrate the relative importance of each term within Eq. 21.

For oil sample, $\partial^2 E_y/\partial x^2$ and $\partial^2 E_y/\partial z^2$ are of the same absolute amplitude. For water, the absolute value of $\partial^2 E_y/\partial x^2$ is negligible compared with the amplitude of $\partial^2 E_y/\partial z^2$ ($\partial^2 E_y/\partial z^2 > 100 \times \partial^2 E_y/\partial x^2$).

For oil sample, differences between 2D numerical simulations and closed-form expressions extended to 2D configurations are explained from the electric field variations along x direction. This leads to amplitude differences and phase shifts between absorbed powers from both approaches.

For water, electric field variations along x direction can be neglected because it does not influence the microwave propagation along z axis. Hence, for a 2D waveguide configuration, the microwave propagation is practically the same as for a 1D configuration problem in the case of water.

For high dielectric materials, the closed-form expressions can predict the microwave absorbed power with a good accuracy either in 1D or 2D configurations (TE_{10} mode). These observations also show that the closed-form expressions extended to 2D geometries are not able to predict the absorbed power within a low dielectric material submitted to an incident sinusoidal wave.

Thermal behavior of water sample

Two-dimensional microwave heating of water sample is simulated for 10 s with initial temperature of 300 K. Calculations are performed on a HPxw4400 Workstation, equipped with Intel® Pentium dual core processor, at 3.4 GHz, with 3 Go of RAM, running on Windows® XP.

Three temperature probes located within the dielectric material are used to follow the thermal behavior of the sample as a function of time.

T_1, T_2, and T_3 are located at 2.5, 7.5, and 12.5 mm, respectively, from the left surface of the sample. Their distribution along the waveguide length corresponds to 44, 27, and 16 mm, respectively (Figure 1).

The heating rate is related to the temperature variations as a function of time. Mathematically, this parameter is defined as follows:

$$\Gamma_i = \left(\frac{\partial T}{\partial t}\right)_i \tag{38}$$

The heat transfer equation is solved numerically using COMSOL®. Two different simulations are performed where the heat source term is calculated either from closed-form expressions or Maxwell's equations approach (Radio-frequency module, 2D). Numerical tests are realized by choosing five sample lengths, respectively, 10, 21, 45, 72, and 103 mm.

Heating rate is calculated for the three temperature probe locations and for each sample length. Results are presented in Table 2 for both approaches.

For all tested sample length, heating rate gives very similar values. The most discrepancies between both simulations are noticed for 21-mm sample depth. However, the relative error is $\sim$10% and it can be neglected regarding the strong influence between the heating rate and the sample length. Consequently, both closed-form expressions and Maxwell's equations approach can predict the thermal behavior of the sample with a good accuracy during 2D microwave heating.

During numerical simulations, computational time plays an important role for the prediction of the thermal behavior of water sample. For a given sample length, the elapsed time is recorded at the end of each numerical simulation.

For both numerical simulations with the two different heat source terms, the computational time increases as a function of sample length (Figure 15). This computational time demand is primarily due to the increase of mesh elements within the 2D geometry. For sample length close to 85 mm, the numerical results show that computational time tends to

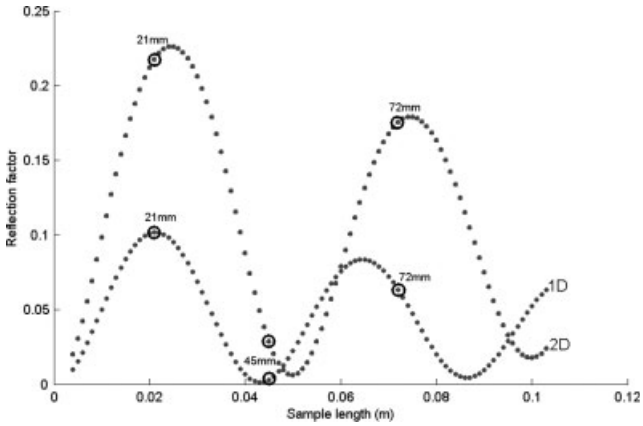

Figure 13. Reflection factor from 1D and 2D numerical simulation as a function of sample length for oil—l_{min} = 0.0138 m, D_p = 0.368 m.

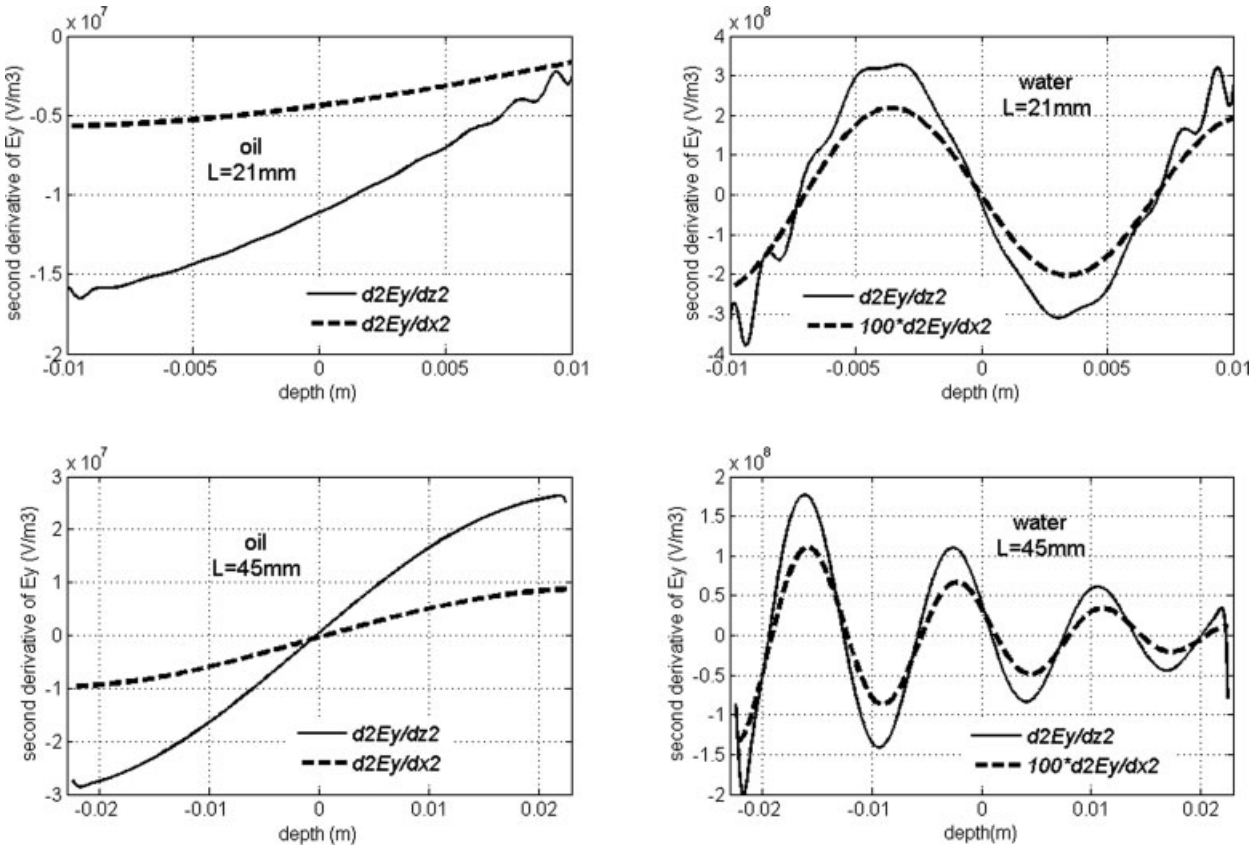

Figure 14. Second derivatives of the electric field for oil and water.

decrease. This phenomenon is primarily due to the mesh adaptation, which is performed during the numerical computation. For sufficiently thick samples, the mesh density in air surrounding medium can be decreased to save computational resources. This adaptation has no effect on the numerical results.

According to our computational resources, the simulation time using Maxwell's equations approach is much bigger than the one from the closed-form relationships. The closed-form relations as a heat source term are able to make a real-time prediction of the temperature rise within the 2D sample. Hence, the best solution is to model 2D microwave heating of high dielectric materials with the closed-form expressions instead of the numerical resolution of Maxwell's equations. The coupling between the heat transfer equation and the closed-form expressions does not require the local electric field computation, i.e., saving of computational time.

Conclusions

Modeling microwave heating is a complex and difficult task as shown by the previous numerical and analytical investigations. This work proposes an extensive study on the influence of the reflection factor value as a function of sample length. Results show quantitatively that sample length plays an important role during the microwave heating process as it can completely change the heating rate within the sample. This study also compares two different approaches dedicated to microwave power calculation. The first one consists in solving numerically the Maxwell's equations using a finite element scheme. The second approach deals with predefined closed-form expressions for microwave power calculation. For 1D configuration problems, results show a very good agreement between both approaches for low and high dielectric materials. The closed-form solutions were initially developed for 1D configuration problems. The originality of

Table 2. Heating Rate as a Function of Sample Length for the Three Temperature Probes

	T_1		T_2		T_3	
	Closed-Form	Numerical	Closed-Form	Numerical	Closed-Form	Numerical
$L = 10$ mm	10°C min^{-1}	10.5°C min^{-1}	3°C min^{-1}	3°C min^{-1}		
$L = 21$ mm	15.5°C min^{-1}	17°C min^{-1}	13°C min^{-1}	15°C min^{-1}	3.5°C min^{-1}	4°C min^{-1}
$L = 45$ mm	10°C min^{-1}	10°C min^{-1}	4.5°C min^{-1}	4.5°C min^{-1}	2°C min^{-1}	2°C min^{-1}
$L = 72$ mm	10.5°C min^{-1}	11°C min^{-1}	5.5°C min^{-1}	5.5°C min^{-1}	2°C min^{-1}	2°C min^{-1}
$L = 103$ mm	10.5°C min^{-1}	11°C min^{-1}	5.5°C min^{-1}	6°C min^{-1}	2°C min^{-1}	2°C min^{-1}

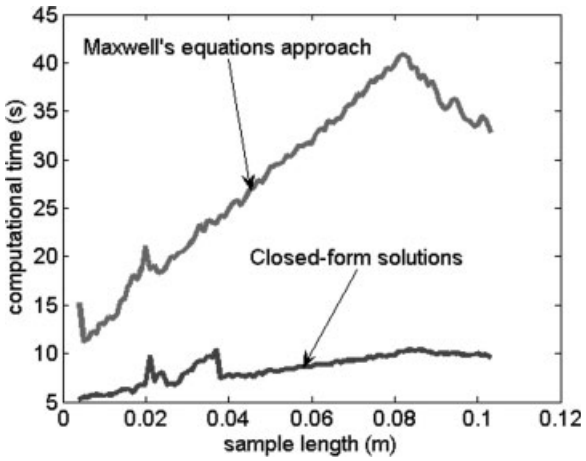

Figure 15. Computational time as a function of sample length.

this work consists in extending those expressions to 2D configuration problems and to compare results with 2D numerical simulation. Thus, for microwave propagation within waveguide structures (2D), closed-form relationships can only be used to predict the microwave absorbed power within high dielectric materials.

According to this analytical approach, both incident electromagnetic field and dielectric properties are the only needed variables to determine the heat source term. Thus, the local electric field strength is not necessary and the heat transfer equation remains the only equation to solve, that is, computational time is reduced.

As a consequence, the closed-form relationships are particularly useful to obtain a quick cartography of the local temperature inside a food sample during 2D microwave heating in TE_{10} fundamental mode. For 2D high dielectric materials, closed-form relationships for microwave power calculation are a promising tool to implement real time control laws dedicated to microwave heating.

Notation

Roman letters

a, b = dimensions of the waveguide, m
A = surface of the quadrilateral mesh, m^2
B = magnetic induction, N s C^{-1} m^{-1}
C_0 = velocity of light in vacuum, m s^{-1}
C_p = specific heat capacity, J kg^{-1} K^{-1}
D_p = penetration depth of the microwaves, m
D = electric displacement, C m^{-2}
E = local electric field amplitude, V m^{-1}
E_0 = maximum amplitude of the incident electric field at left side, V m^{-1}
E_{in} = incident electric field at left side, V m^{-1}
E_c = total electric field strength on excitation port
E_1 = electric field pattern on excitation port 1
f = frequency of the electromagnetic wave, Hz
f_c = cutoff frequency, Hz
F_0 = incident microwave power flux at left side, W m^{-2}
h = convective heat transfer coefficient, W m^{-2} K^{-1}
H = magnetic field intensity, A m^{-1}
J = current flux, A m^{-2}
k = thermal conductivity, W m^{-1} K^{-1}
l_{min} = upper bound limit for thin sample asymptote, m
L = thickness of the sample, m
$l_1 \ldots l_4$ = side lengths for the quadrangle mesh, m
P_{in} = incident microwave power, W
$P_{reflected}$ = reflected microwave power, W
$P(t)$ = Poynting vector in the time domain
Q = volumetric heat generation term, W m^{-3}
S = left surface of the sample, m^2
T = temperature, K
T_0 = initial temperature of product, K
T_∞ = external temperature, K
x, y, z = spatial coordinates, m
Z_0 = free space impedance of electromagnetic wave, Ω
$Z_{TE\ 0}$ = impedance of electromagnetic wave within air in waveguide, Ω
Z_{sample} = impedance of electromagnetic wave within semi-infinite sample, Ω
$Z_{TE\ sample}$ = impedance of electromagnetic wave within sample in waveguide, Ω.

Greek letters

λ_0 = free space wavelength, m
λ_c = cutoff wavelength, m
λ_{g0} = guided wavelength, m
λ_m = wavelength within dielectric medium, m
κ_i = complex propagation constant within ith medium
κ_{ia} = real part of κ_i, m^{-1}
κ_{ib} = imaginary part of κ_i, m^{-1}
ω = pulsation of the microwave radiation, rad s^{-1}
μ = magnetic permeability of the material, H m^{-1}
μ_0 = magnetic permeability of vacuum (1.256×10^{-6} H m^{-1})
ε_0 = permittivity of vacuum (8.85×10^{-12} F m^{-1})
ε_r = complex permittivity (dimensionless)
ε_r' = relative dielectric constant (dimensionless)
ε_r'' = relative dielectric loss factor (dimensionless).

Literature Cited

1. Metaxas AC. *Foundations of Electroheat: A Unified Approach*. Chichester, U.K.: Wiley, 1996.
2. Ayappa KG. Microwave heating: an evaluation of power formulations. *Chem Eng Sci*. 1991;46:1005–1016.
3. Basak T. Role of resonances on microwave heating of oil-water emulsions. *AIChE J*. 2004;50:2659–2675.
4. Basak T. Analysis of resonances during microwave thawing of slabs. *Int J Heat Mass Transfer*. 2003;46:4279–4301.
5. Curet S, Rouaud O, Boillereaux L. Microwave tempering and heating in a single-mode cavity: numerical and experimental investigations. *Chem Eng Process*. 2008;47:1656–1665.
6. Ratanadecho P, Aoki K, Akahori M. A numerical and experimental investigation of the modelling of microwave melting of frozen packed beds using a rectangular wave guide. *Int Commun Heat Mass Transfer*. 2001;28:751–762.
7. Chamchong M, Datta AK. Thawing of foods in a microwave oven. I. Effect of power levels and power cycling. *J Microwave Power Electromagn Energy*. 1999;34:22–32.
8. Chatterjee S, Basak T, Das SK. Microwave driven convection in a rotating cylindrical cavity: a numerical study. *J Food Eng*. 2007;79:1269–1279.
9. Herve AG, Tang J, Luedecke L, Feng H. Dielectric properties of cottage cheese and surface treatment using microwaves. *J Food Eng*. 1998;37:389–410.
10. Oliveira MEC, Franca AS. Microwave heating of foodstuffs. *J Food Eng*. 2002;53:347–359.
11. Dincov DD, Parrott KA, Pericleous KA. Heat and mass transfer in two-phase porous materials under intensive microwave heating. *J Food Eng*. 2004;65:403–412.
12. Geedipalli SSR, Rakesh V, Datta AK. Modeling the heating uniformity contributed by a rotating turntable in microwave ovens. *J Food Eng*. 2007;82:359–368.
13. Rattanadecho P. The simulation of microwave heating of wood using a rectangular wave guide: influence of frequency and sample size. *Chem Eng Sci*. 2006;61:4798–4811.

14. Rattanadecho P, Aoki K, Akahori M. A numerical and experimental investigation of the modelling of microwave heating for liquid layers using a rectangular wave guide (effects of natural convection and dielectric properties). *Appl Math Modell*. 2002;26:449–472.
15. Vegh V, Turner IW, Zhao H. Effective cell-centred time-domain Maxwell's equations numerical solvers. *Appl Math Modell*. 2005;29: 411–438.
16. Zhao H, Turner IW. The use of a coupled computational model for studying the microwave heating of wood. *Appl Math Modell*. 2000;24:183–197.
17. Bhattacharya M, Basak T. On the analysis of microwave power and heating characteristics for food processing: asymptotes and resonances. *Food Res Int*. 2006;39:1046–1057.
18. Bhattacharya M, Basak T. A novel closed-form analysis on asymptotes and resonances of microwave power. *Chem Eng Sci*. 2006;61:6273–6301.
19. Bhattacharya M, Basak T. New closed form analysis of resonances in microwave power for material processing. *AIChE J*. 2006;52: 3707–3721.
20. Ayappa KG, Davis HT, Davis EA, Gordon J. 2 Dimensional finite-element analysis of microwave heating. *AIChE J*. 1992;38:1577–1592.
21. Lanz JE. *A Numerical Model of Thermal Effects in a Microwave Irradiated Catalyst Bed*. Blacksburg, VA: Virginia Polytechnic Institute and State University, 1998.
22. Zhu J, Kuznetsov AV, Sandeep KP. Mathematical modeling of continuous flow microwave heating of liquids (effects of dielectric properties and design parameters). *Int J Therm Sci*. 2007;46:328–341.
23. Arunachalam K, Melapudi VR, Udpa L, Udpa SS. Microwave NDT of cement-based materials using far-field reflection coefficients. *NDT E Int*. 2006;39:585.
24. Jolly P, Turner I. Non-linear field solution of one-dimensional microwave heating. *J Microwave Power Electromagn Energy*. 1990; 25:3–15.
25. Barringer SA, Davis EA, Gordon J, Ayappa KG, Davis HT. Effect of sample size on the microwave heating rate: oil vs. water. *AIChE J*. 1994;40:1433–1439.
26. Buffler CR. *Microwave Cooking and Processing*. New York: Van Nostrand Reinhold, 1993.
27. Taher BJ, Farid MM. Cyclic microwave thawing of frozen meat: experimental and theoretical investigation. *Chem Eng Process*. 2001; 40:379–389.
28. Akkari E, Chevallier S, Boillereaux L. A 2D non-linear "grey-box" model dedicated to microwave thawing: theoretical and experimental investigation. *Comput Chem Eng*. 2005;30:321–328.
29. Metaxas AC, Meridith RJ. *Industrial Microwave Heating*. London: Peter Peregrinus, 1983.
30. Brodie G. *Microwave Timber Heating and its Application to Solar Drying*. Institute of Land and Food Resources, University of Melbourne; 2005.
31. Saltiel C, Datta AK. Heat and mass transfer in microwave processing. *Adv Heat Transfer*. 1999;33:1–94.
32. Ayappa KG, SenGupta T. Microwave heating in multiphase systems: evaluation of series solutions. *J Eng Math*. 2002;44:155–171.

Appendix

Analytical Expressions Dedicated to Microwave Power Calculation

The following expressions are needed to compute the microwave absorbed power within the sample for both thick sample regime and resonating regime.

$$\kappa_i = \kappa_{ia} + j\kappa_{ib} = \frac{2\pi}{\lambda_i} + j\frac{1}{(D_p)_i}$$

$$p = \frac{\kappa_{1a}}{\kappa_{2a}}$$

$$n = \frac{\kappa_{2b}}{\kappa_{2a}}$$

$$\delta_{ij}^R = \kappa_{ia}\kappa_{ja} + \kappa_{ib}\kappa_{jb} \quad i,j = 1,2,3,$$

$$C^- = c_1\cos(\kappa_{2a}L(1-z'))) + c_2\cos h(\kappa_{2b}L(1-z'))) + c_3\sin(\kappa_{2a}L(1-z'))) + c_4\sin h(\kappa_{2b}L(1-z')))$$

$$C^d = \left(c_3^2 - c_1^2\right)\cos(2\kappa_{2a}L) + \left(c_2^2 + c_4^2\right)\cos h(2\kappa_{2b}L) - 2c_1c_3\sin(2\kappa_{2a}L) + 2c_2c_4\sin h(2\kappa_{2b}L)$$

$$c_1 = \kappa_{2a}^2 + \kappa_{2b}^2 - \kappa_0^2$$

$$c_2 = k_{2a}^2 + \kappa_{2b}^2 + \kappa_0^2$$

$$c_3 = -2\kappa_0\kappa_{2b}$$

$$c_4 = 2\kappa_0\kappa_{2a}$$

Manuscript received Mar. 27, 2008, revision received Sept. 17, 2008, and final revision received Nov. 21, 2008.